La-doped $BiFeO_3$: Synthesis and multiferroic property study

Lin Peng-Ting(蔺鹏婷)[a], Li Xiang(李 祥)[a)†], Zhang Li(张 丽)[a], Yin Jin-Hua(阴津华)[b], Cheng Xing-Wang(程兴旺)[a], Wang Zhi-Hong(王志宏)[c], Wu Yu-Chuan(吴玉娟)[d], and Wu Guang-Heng(吴光恒)[c]

[a] *School for Materials Science and Engineering, Beijing Institute of Technology, Beijing* 100081, *China*
[b] *Physics Department, University of Science & Technology of Beijing, Beijing* 100083, *China*
[c] *State Key Laboratory of Magnetism, Institute of Physics, Chinese Academy of Sciences, Beijing* 100190, *China*
[d] *Department of Materials and Mineral Resources Engineering, National Taipei University of Technology, Taiwan, China*

(Received 25 September 2013; revised manuscript received 30 October 2013; published online 20 February 2014)

A new sol-foam-gel method was developed to fabricate La-doped $BiFeO_3$ multiferroic materials. It was demonstrated that a gradual increase in the content of La-doped into $BiFeO_3$ results in its structure changing from rhombohedral to orthorhombic. A study of other property changes indicates that La-doping in $BiFeO_3$ enhances its ferromagnetism and ferroelectricity. A temperature-dependent magnetization study suggests that the magnetic property of La-doped $BiFeO_3$ samples varied from antiferromagnetic to ferromagnetic as the content of La-doped into $BiFeO_3$ increased from 0 to 20%. Unique temperature-dependent zero field cooling (ZFC) and field cooling (FC) magnetization behaviors were observed in 15% La-doped $BiFeO_3$ — its ZFC temperature-dependent magnetization being ferromagnetic and its FC temperature-dependent magnetization being antiferromagnetic. A possible mechanism of such an interesting M–T behavior is discussed.

Keywords: multiferroic, $BiFeO_3$, ferromagnetism

PACS: 77.80.Dj, 77.84.–s, 81.20.Ka **DOI:** 10.1088/1674-1056/23/4/047701

1. Introduction

Multiferroic materials, in which ferromagnetic, ferroelectric, and/or ferroelastic orderings coexist, have attracted much attention in recent years.[1–6] The unique property of multiferroic materials supplies them with a magneto–electric (ME) effect in which the magnetization can be tuned by an applied electric field and *vice versa*. Hence, multiferroic materials offer wide applications, such as spintronics, new data storage media, and ferroelectric random-access memories.[7,8]

$BiFeO_3$ (BFO), one of the single-phase multiferroic materials at room temperature (RT), exhibits the coexistence of ferroelectric ordering with Curie temperature (T_C) of 850 °C and antiferromagnetic (AFM) ordering with a Nèel temperature (T_N) of 370 °C.[9] At room temperature, bulk BFO has the rhombohedral, distorted perovskite structure with space group $R3C$ ($a = 5.63$ Å and $\alpha = 59.35°$). The magnetic structure of BFO is G-type antiferromagnetism with a superimposed incommensurate cycloid spin structure, and the periodicity of the cycloid spin structure is 62 nm. Such a unique spin structure inhibits the observation of the linear magnetoelectric effect in BFO ceramics.[9,10] Much effort has been made to improve the magnetic properties of BFO by substituting rare-earth ions[11–19] or alkaline-earth ions[20,21] for the A-site ions and by substituting transition metal ions for the B-site ions.[22–25] The achieved results demonstrate that A-site or B-site doping in BFO is an effective way to enhance its magnetic properties and to reduce its leakage current. The reduction of leakage current is critical to switching the ferroelectric polarization in the doped BFO.

Despite extensive study, the origin of the enhanced magnetization in doped BFO is still an issue of debate: both the chemical valence fluctuation of Fe ions and the broken cycloid spin structure in the doped BFO are supposed to be the reason for such a magnetization increase.

In this paper, a modified sol-foam-gel method, namely, the sol-foam-gel route, was developed to fabricate La-doped BFO with a nominal composition of $Bi_{1-x}La_xFeO_3$ (BL_xFO) ($x = 0.05$, 0.10, 0.15, 0.20). The structure, ferromagnetism, and ferroelectricity of the produced samples were studied.

2. Experiment

Ceramic samples of BL_xFO ($x = 0$, 0.05, 0.10, 0.15, 0.20) were synthesized by the sol-foam-gel route. Stoichiometric $Bi(NO_3)_3{\cdot}5H_2O$, $La(NO_3)_3{\cdot}6H_2O$, and $Fe(NO_3)_3{\cdot}9H_2O$ were selected as precursors and dissolved in acetic acid and distilled water. A 5-mol% excess bismuth nitrate was added to compensate for the Bi loss during the thermal treatment. Citric acid (molar ratio of metal to tartaric acid=2:1) was added to obtain a clear yellow-colored solution. The mixture solution was stirred for several hours at 80 °C. Thereafter, the precursor solution was evaporated and dried in an oven at 130 °C to obtain the foam gel. Then the gel was ground into powder and calcined at 500 °C for 4 h. The calcined powders were fine milled and pressed into 1-mm-thick disks 10 mm in diameter. Finally, all the samples were sintered at 800 °C for 6 h. For electrical measurement, the ceramic samples were polished to 0.2-mm thickness and painted with silver as electrode on both

†Corresponding author. E-mail: aihyoo@bit.edu.cn

© 2014 Chinese Physical Society and IOP Publishing Ltd

surfaces.

The structural characterization was done by powder X-ray diffraction (XRD) using θ–2θ scans with Cu Kα radiation. The magnetic properties were measured using a vibrating sample magnetometer. The ferroelectric hysteretic loops and the leakage current density–time (J–T) characteristics were obtained using a ferroelectric Analyzer. X-ray photoelectron spectroscopy (XPS) was used to examine the chemical state of Fe ions in the samples.

3. Result and discussion

Figure 1 shows the XRD patterns of $Bi_{1-x}La_xFeO_3$ (x = 0, 0.05, 0.1, 0.15, 0.2) ceramic samples sintered at 800 °C. As shown in Fig. 1, for BFO samples, all the detectable XRD patterns match to the distorted rhombohedral $R3C$ structure. However, a small amount of impurity phase was observed, which can be identified as $Bi_2Fe_4O_9$.[11] The impurity phase disappeared rapidly in the $Bi_{1-x}La_xFeO_3$ samples as the La content gradually increases. This result suggests that La doped into BFO suppresses the impurity phase effectively. Compared with the XRD patterns of $Bi_{1-x}La_xFeO_3$ ($x = 0 \sim 0.2$) in Fig. 1, the structures of the substituted samples changed significantly. In detail, for $Bi_{1-x}La_xFeO_3$ (x = 0.1, 0.15, and 0.2), the diffraction peaks (021) and (024) are split; while the (104) and (110) peaks merge into one peak. These results suggest that the structure of the $Bi_{1-x}La_xFeO_3$ changes from rhombohedral to orthorhombic, in which the corresponding space group changed from $R3C$ to $C222$, agreeing with previous reports on rare-earth-doped $BiFeO_3$ materials.[15,16,19,25] The structural study indicates that the sol-foam-gel route is an effective way to synthesize La-doped $BiFeO_3$ bulk materials.

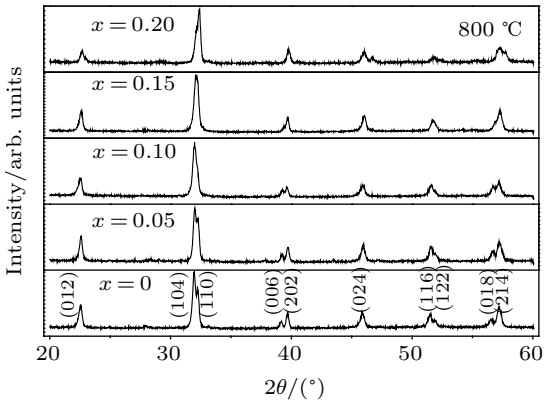


Fig. 1. XRD patterns of $Bi_{1-x}La_xFeO_3$ (x = 0, 0.05, 0.10, 0.15, 0.20) sintered at 800 °C.

Figure 2 illustrates RT applied magnetic field-dependent magnetization (M–H) loops of $Bi_{1-x}La_xFeO_3$ (x = 0, 0.05, 0.10, 0.15, 0.20) ceramics sintered at 800 °C. For the x = 0 sample, no M–H loop was observed, which reveals that this sample is antiferromagnetic, agreeing with the previous reports.[26,27] However, for $Bi_{1-x}La_xFeO_3$ ceramics, their M–H loops become more and more prominent as the doped La content increases from x = 0.05 to x = 0.20. The remanent magnetization (M_r) is 0.0158, 0.0053, 0.0335 emu/g for x = 0.05, 0.10, and 0.15, respectively. Compared with $BiFeO_3$ and $Bi_{0.95}La_{0.05}FO_3$, one sees that the magnetization of $Bi_{0.95}La_{0.05}FO_3$ is a little smaller than that of BFO. Considering the different characteristic of the XRD patterns of $Bi_{0.95}La_{0.05}FeO_3$ and BFO, it is reasonable to believe that the reduced magnetization of $Bi_{0.95}La_{0.05}FO_3$ could result from a suppression of the paramagnetic $Bi_2Fe_4O_9$ in La-doped BFO.[13] Another characteristic of M–H for $Bi_{1-x}La_xFeO_3$ (x = 0.05–0.15) is that no saturation magnetization was observed, demonstrating that large portions of an antiferromagnetic or paramagnetic phase exist in the $Bi_{1-x}La_xFeO_3$ samples.[28]

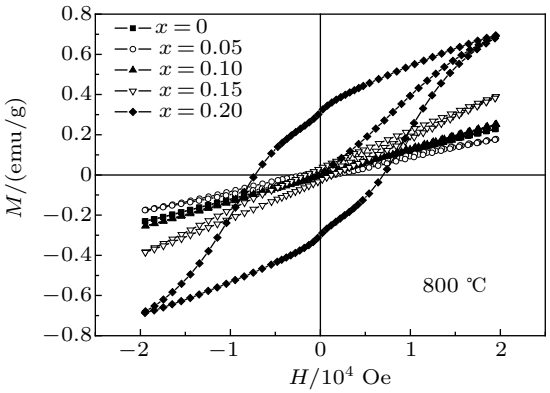


Fig. 2. Magnetization as a function of applied field (M–H) at room temperature of $Bi_{1-x}La_xFeO_3$ (x = 0, 0.05, 0.1, 0.15, and 0.20) sintered at 800 °C.

Interestingly, for $Bi_{0.8}La_{0.2}FeO_3$, a large M–H loop is observed with M_r of 0.3167 emu/g and coercivity of 7421 Oe (1 Oe = 79.5775 A·m^{-1}). Furthermore, a kink was observed in the M–H loop of $Bi_{0.8}La_{0.2}FeO_3$, which suggests that two coupled magnetic phases exist in this sample, as indicated in the previous study on double phase permanent magnets.[29] The significant increase of the magnetization in the $Bi_{0.8}La_{0.2}FeO_3$ sample could result from the breaking of its spin cycloid structure and the latent magnetization locked within the cycloid released.[6]

Previous studies on solid phase reaction-synthesized $Bi_{0.8}La_{0.2}FeO_3$ by Zhang S T *et al.*[12] and Das S R *et al.*[30] suggested that its M_r is 0.0042 emu/g and 0.075 emu/g respectively, much smaller than our findings. This implies that our sol-foam-gel method is effective in the synthesis of La-doped $BiFeO_3$ with a sufficiently enhanced ferromagnetic property. With detailed analysis, we found that the M–H loops of $Bi_{0.85}La_{0.15}FeO_3$ and $Bi_{0.8}La_{0.2}FeO_3$ (shown in Fig. 2) are shifted in the horizontal and vertical directions, revealing that an AFM–FM coupling exists in these samples, with exchange fields of −133 Oe and −110 Oe, respectively.

Figures 3(a)–3(d) show the temperature-dependent magnetization (M–T) of $Bi_{1-x}La_xFeO_3$ ($x = 0$, 0.05, 0.15, and 0.2) samples, after field cooling (FC) and zero field cooling (ZFC). The measured temperature is in the range of 400 K to 60 K, the cooling field is 10 kOe and the measurement field is 100 Oe. Compared with the M–T characteristics of different samples, the magnetization of BFO is little larger than that of $Bi_{0.95}La_{0.05}FeO_3$, while the magnetizations of $Bi_{0.85}La_{0.15}O_3$ and $Bi_{0.8}La_{0.2}O_3$ are much larger than that of BFO. These results agree well with the results of our M–H study shown in Fig. 2.

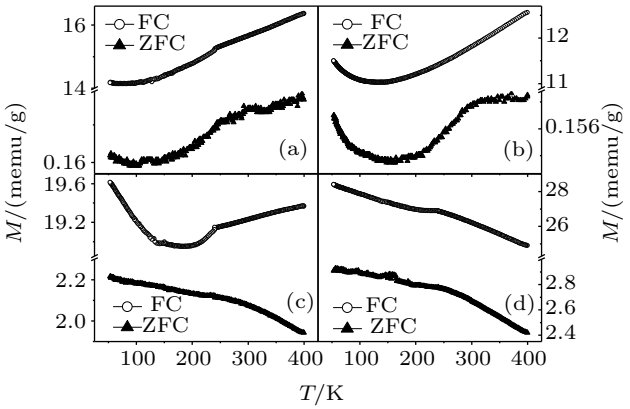


Fig. 3. Temperature-dependent field-cooling and zero-field cooling magnetizations of $Bi_{1-x}La_xFO_3$ sintered at 800 °C: (a) $x = 0$; (b) $x = 0.05$; (c) $x = 0.15$; (d) $x = 0.20$.

Figure 3(a) reveals that the magnetization of the BFO sample decreased as the temperature decreased down to 100 K, as shown on both ZFC and FC M–T curves, suggesting a typical AFM property. A drastic decrease of magnetization observed in the M–T curve near 260 K could be induced by the impurity $Bi_2Fe_4O_9$, since $Bi_2Fe_4O_9$ has a magnetic phase transition from high temperature paramagnetism to low temperature antiferromagnetism near 260 K.[31] However, when the temperature decreases from 100 K to 60 K, the magnetization of BFO shows a little increase, which could result from the fractional ferromagnetic phase existing in the BFO sample at this temperature range, agreeing with the reported studies.[14,22,32]

Figure 3(b) shows the ZFC and FC M–T curves of $Bi_{0.95}La_{0.05}FeO_3$, similar to those of BFO. However, some different characteristics are prominent. First, the drastic decrease of magnetization that is observed on the ZFC curve near 260 K in the BFO sample disappears on that of the $Bi_{0.95}La_{0.05}FeO_3$ sample, demonstrating the suppression of $Bi_2Fe_4O_9$ in this sample. Second, the transition temperature between the antiferromagnetic and ferromagnetic in $Bi_{0.95}La_{0.05}FeO_3$ is observed near 150 K, while a similar antiferromagnetic–ferromagnetic transition in BFO was observed near 100 K, suggesting that doping of La into BFO induces this rise in transition temperature.

Figure 3(c) shows the ZFC and FC M–T curves of $Bi_{0.85}La_{0.15}FeO_3$. The ZFC M–T indicates that the magnetization increases as the temperature decreases, a typical ferromagnetic property. Surprisingly, the FC M–T curve of $Bi_{0.85}La_{0.15}FeO_3$ reveals that the magnetization of this sample decreases as the temperature decreases down to 250 K, very slowly increases in the range of 250 K to 150 K, and then quickly increases as the temperature decreases further. Such a characteristic indicates that after 10-kOe field cooling, a phase transition happens from antiferromagnetic to ferromagnetic in the range of 250 K $\sim$ 150 K in this sample. The unique characteristic of the FC M–T of the $Bi_{0.85}La_{0.15}FeO_3$ sample suggests that a competition between the ferromagnetism and antiferromagnetism could exist in this sample, as indicated in the previous reports on $NdFeO_3$.[13] Another characteristic of the FC M–T of this sample is that the transition temperature between ferromagnetic to antiferromagnetic is located near 200 K, much higher than that in BFO and $Bi_{0.95}La_{0.05}FeO_3$. Furthermore, the magnetization of the low temperature ferromagnetic phase is enhanced significantly compared with that of the BFO and $Bi_{0.95}La_{0.05}FeO_3$ samples. Figure 3(d) shows the ZFC and FC M–T curves of $Bi_{0.8}La_{0.2}FeO_3$, which demonstrate that this sample is ferromagnetic. As suggested previously, the spin cycloid structure can be destroyed by La-doping, the latent magnetization locked within the cycloid structure is released and the samples become ferromagnetically ordered.[6] Compared with different characteristics of ZFC and FC M–T in Fig. 3, one sees that the transition temperature of antiferromagnetic to ferromagnetic in La-doped samples increases as the doped La content increases, and finally, the sample is ferromagnetic at RT, as indicated in Fig. 3(d).

To further understand the unexpected characteristic FC M–T of the $Bi_{0.85}La_{0.15}FeO_3$ sample, one should keep in mind that a weak exchange bias field of -140 Oe and -118 Oe is observed in the $Bi_{0.85}La_{0.15}FeO_3$ and $Bi_{0.8}La_{0.2}FeO_3$ samples, as indicated in Fig. 2, while a small vertical shift of M–H loops with $\Delta M_r = (M_{r+} - M_{r-})$ of 0.0048 emu/g and 0.013 emu/g is also observed in these samples. Such results suggest that AFM and FM phases co-exist in both samples. As is known, the existence of the exchange bias field and the small vertical shift of M–H loops together imply that uncompensated spins exist in the interfaces between AFM and FM phases and that the unidirectional magnetism formed in the samples.[33] Therefore, the unique FC M–T behavior in $Bi_{0.85}La_{0.15}FeO_3$ can be understood in the view presented below. In the ZFC M–T, the spin directions of AFM domains in the sample are distributed randomly. In this case, the coefficient of the temperature-dependent magnetic susceptibility is very small.[34] Therefore, the AFM phase in the studied sample contributes nearly nothing to its temperature-dependent magnetization. Accordingly,

the M–T behavior in ZFC is due to the increase in the magnetization of the ferromagnetic phase in the studied sample. However, in FC, the spin direction of the AFM domains in the sample turns to the direction of an applied field. Consequently, AFM domains in the FC processing have a much larger coefficient of temperature-dependent magnetic susceptibility, resulting in the drastic magnetization decrease as the temperature decreases. Thus, the antiferromagnetic M–T behavior of the FC processing (Fig. 3(c) in the range of 300 K $\sim$ 250 K) is induced by the contribution of the AFM and FM phases, considering the larger coefficient of the temperature-dependent magnetic susceptibility of the AFM phase and the small coefficient of the temperature-dependent magnetic susceptibility of the FM phase. With temperature decreasing much more, ferromagnetic coupling in the ferromagnetic phase increases and results in ferromagnetism dominating in $Bi_{0.85}La_{0.15}FeO_3$.[34]

Based upon the RT M–H loop measurements as well as ZFC M–T and FC M–T study results, we find that the ferromagnetic phase becomes more and more dominant as the content of La doped in the studied samples increases. The increase of the ferromagnetic phase in the studied sample will induce an increase of the interfacial interaction between AFM and FM; thus, the spin direction of the FM phase will be pinned by the AFM domains, resulting in the observation of exchange bias fields. The spin pinning effects in the interfaces of AFM and FM phase will also effectively modify the ZFC and ZF M–T behaviors of the studied samples, i.e., the AFM domains' distribution will modulate the spin direction of the FM phase, finally resulting in the distinctly different ZFC M–T and FC M–T behaviors.

Figure 4 illustrates RT applied electrical field-dependent ferroelectric hysteretic (P–E) loops of $Bi_{1-x}La_xFeO_3$ (x = 0.00, 0.05, 0.10, 0.15, 0.20) ceramics sintered at 800 °C. Figure 4 indicates that for $BiFeO_3$ and $Bi_{0.95}La_{0.05}O_3$ samples, the P–E loops are shaped elliptically, which indicates that these samples have much high leakage current, resulting in the failure of the applied electrical field-stimulated ferroelectric polarization rotation. With the doped La amounting to more than $x = 0.1$ in the samples, the prominent P–E loops obtained under the applied electrical field have different frequencies. The remnant polarization values and the coercive fields are 3.42, 6.95, 3.32, 2.97 μC/cm^2 and 14.01, 8.95, 17.33, 28.67 kV/cm for $Bi_{1-x}La_xFeO_3$ with $x = 0.05$, 0.1, 0.15, and 0.20, respectively. These results reveal that increasing the content of doped La less than $x = 0.1$ in BFO induces a remnant polarization increase; nevertheless, the remnant polarization decreases when the doped La content is larger than $x = 0.1$ for the corresponding samples. Furthermore, with increasing the La content in BFO, the coercive fields of the corresponding sample increase.

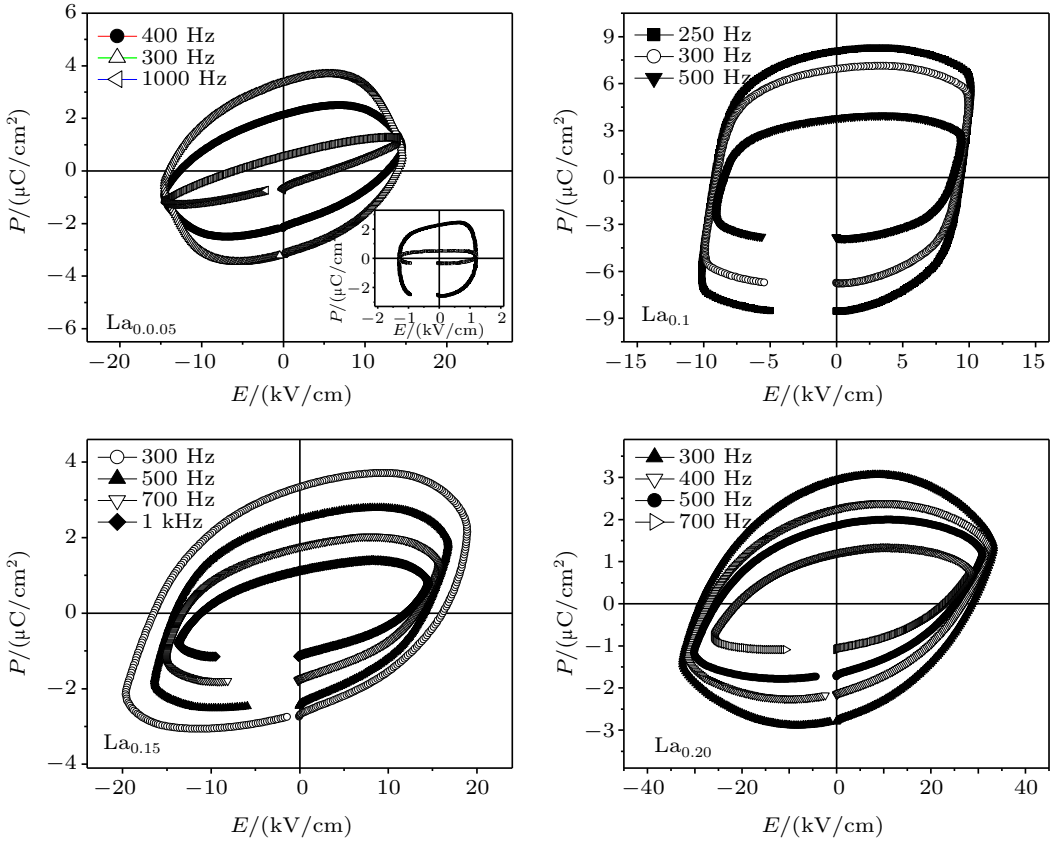


Fig. 4. Ferroelectric hysteretic loops of La-doped $BiFeO_3$ sintered at 800 °C.

Figure 5 shows the Fe 2p XPS spectra of $Bi_{1-x}La_xFeO_3$ ($x = 0$, 0.05, 0.1, 0.15, 0.2) samples sintered at 800 °C, in which the binding energy of Fe $2p_{3/2}$ increases from 709 eV to 711.4 eV as the content of the doped La increases from $x = 0$ to 0.15. It has been known that the binding energies of Fe^{3+} $2p_{3/2}$ and Fe^{2+} $2p_{3/2}$ are 711 eV and 709.5 eV, respectively.[26,35] Therefore, XPS results confirm that Fe^{2+} ions exist in the BFO sample; however, Fe^{2+} concentration is suppressed as the content of the doped La in the studied samples increases. It is especially interesting that nearly no trace of Fe^{2+} is observed for $x = 0.10$, 0.15 samples, consistent with the Simões *et al.* report.[36] Nevertheless, with the concentration of doped La increased to $x = 0.2$, the binding energy of Fe $2p_{3/2}$ decreases to 711 eV, which could result from a complete structure transition from rhombohedral to orthorhombic, as indicated in the XRD characterization shown in Fig. 1. The structural transition causes a change of the chemical environment of Fe ions, and thus, a change of Fe ion chemical charge states.

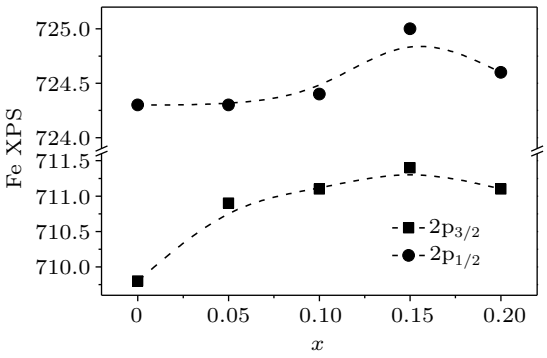


Fig. 5. XPS spectra of $Bi_{1-x}La_xFeO_3$ ($x = 0$, 0.05, 0.1, 0.15, 0.2) sintered at 800 °C.

Figure 6 shows the time-dependent leakage current of $Bi_{1-x}La_xFeO_3$ ($x = 0$, 0.05, 0.15, 0.20) ceramics samples sintered at 800 °C. Figure 6(a) is the measured leakage current curves as a function of time, and figure 6(b) is the normalized curves for the corresponding samples. From Fig. 6, one can see that the leakage current of all the samples decayed exponentially. A careful analysis indicates that the leakage current of $Bi_{0.95}La_{0.05}FeO_3$ is drastically reduced by a few orders as compared with that of BFO. However, the leakage current of $Bi_{0.85}La_{0.15}FeO_3$ is much larger than that of $Bi_{0.95}La_{0.05}FeO_3$ but smaller than that of BFO, while the leakage current of $Bi_{0.80}La_{0.20}FeO_3$ is markedly smaller than that of $Bi_{0.95}La_{0.05}FeO_3$. Therefore, it is particularly interesting that the leakage current does not decrease monotonically with an increase of the doped La in BFO, although it is believed that doping of lanthanides can suppress the formation of oxygen vacancies in doped samples, consistent with the previous studies on Gd-doped BFO films.[37] Figure 6(b) suggests that the doping of La in BFO not only reduces the leakage current of the corresponding sample, but also enhances the decay rate of the leakage current. Previous studies demonstrated that the leakage current in BFO originates from the oxygen vacancies or the chemical valence fluctuation of iron between Fe^{3+} and Fe^{2+}. Thus, figure 6 confirms that a small amount of La doped in BFO induces less fluctuation in the Fe chemical valences, reduced drastically in the corresponding samples, consistent with previous reports.[30,38,39] While an increase of the content of the doped La in BFO induces the leakage current to increase a little, but still much smaller than that of BFO. Such a small increase in leakage current could be induced by the change of bond lengths and angles of BLFO. In the highly La-doped BFO, the structural transition releases the distortion or strains of the bonds, which could result in reducing its leakage current. This supposition is confirmed by the XRD and XPS studies, as shown in Fig. 2 and Fig. 5.

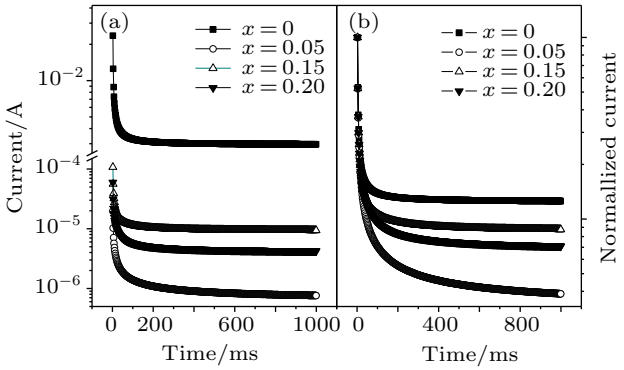


Fig. 6. Time-dependent leakage current of $Bi_{1-x}La_xFeO_3$ ($x = 0$, 0.05, 0.1, 0.15, 0.2) sintered at 800 °C.

The origin of the ferromagnetism in BFO is a subject of debate. The interaction between Fe^{2+} and Fe^{3+}[40] or the spin canting in the unit cell of BFO contribute to the magnetism of BFO or doped BFO samples.[14] In this work, we demonstrated that a very small amount of La doped in BFO reduces its Fe^{2+} concentration, while no prominent reduction of the ferromagnetism is observed in the corresponding samples, as indicated in Fig. 2. Whereas in highly La-doped samples, the density of Fe^{2+} is much lower than that in BFO, as indicated by our XPS study (Fig. 5), and distinctive ferromagnetism is observed, as confirmed by the *M*–*H* loop shown in Fig. 2. Therefore, we deduce that the prominent ferromagnetism in La-doped BFO is due not to the interaction between Fe^{3+} and Fe^{2+} but to its structure distortion or transition, which breaks its spin cycloid structure and releases the latent magnetization locked within BFO.

The Landau–Ginzburg theory indicates that the destruction of the spin cycloid of $BiFeO_3$ leads to enhanced magnetic-electric (ME) coupling and improves the material's multiferroicity effectively.[41,42] Thus, the abrupt increase in magnetization and polarization, as shown in Fig. 4(b) and Fig. 2, should be attributed directly to the enhancement of ME coupling by the destruction of the spin cycloid. The intrinsic reasons for the enhancement of the magnetization in La-doped

$BiFeO_3$ could be understood as follows: first, La-doping of BFO leads to lattice distortion and a variation of the canting angle of the Fe–O–Fe bond. Consequently, the latent spins are blocked in La-doped BFO releases. Second, La-doping of BFO will induce La- and Fe-related magnetic sublattices, and these two sublattices could have some magnetic coupling that enhances BFO's ferromagnetic property, as indicated by the ZFC and FC M–T measurement results shown in Fig. 3, consistent with the reports by Zhang *et al*.[14]

4. Conclusion

We demonstrated that La-doped BFO (BLFO) synthesized by our sol-foam-gel related method is a distinctive multiferroic material. La-doping of BFO suppresses the impurity phases. However, ferromagnetic and antiferromagnetic phases were found to exist in the studied samples even though the XRD results demonstrate no trace of impurity phase structures. The ferromagnetic and ferroelectric characteristics coexist in $Bi_{1-x}La_xFeO_3$ ($x = 0.15$, 0.2) at room temperature. The enhanced ferromagnetism in La-doped BFO results from the breaking of its spin cycloid structure by the La-doping-induced structural distortion or phase transition.

References

[1] Kimura T, Goto T, Shinatanni H, Ishizaka K, Arima T and Tokura Y 2003 *Nature* **42** 655

[2] Wu S M, Cybart S A, Yi D, Parker J M, Ramesh R and Dynes R C 2013 *Phys. Rev. Lett.* **110** 067202

[3] Matsuda M, Fishman R S, Lee C H, Ushiyama T, Yanagisawa Y and Ito T 2012 *Phys. Rev. Lett.* **109** 067205,

[4] Li J B, Rao G H, Xiao Y H, Luo J, Liu G Y, Chen J R and Liang J K 2010 *Chin. Phys. B* **19** 107505

[5] Prelier W, Singh M P and Murugavel P 2005 *J. Phys.: Condens. Matter* **17** 803

[6] Wang K F, Liu J M and Ren Z F 2009 *Adv. Phys.* **58** 4

[7] Hill N A 2000 *J. Phys. Chem. B* **104** 6694

[8] Fiebig M, Lottermoser Th, Fröhlich D, Goltsev A V and Pisarev R V 2002 *Nature* **419** 818

[9] Fischer P, Polomska M, Sosnowska I and Szymański M 1980 *J. Phys. C: Solid State Phys.* **13** 1931

[10] Sosnowska I, Peterlin-Neumaier T and Steichele E 1982 *J. Phys. C: Solid State Phys.* **15** 4835

[11] Yan X L, Chen J G, Qi Y F, Cheng J R and Meng Z Y 2010 *J. Eur. Ceram. Soc.* **30** 265

[12] Zhang S T, Zhang Y, Lu M H, Du C L, Chen Y F, Liu Z G, Zhu Y Y and Ming N B 2006 *Appl. Phys. Lett.* **88** 162901

[13] Cheng Z X, Li A H, Wang X L, Dou S X, Ozawa K, Kimura H, Zhang S J and Shrout T R 2008 *J. Appl. Phys.* **103** 07E507

[14] Zhang Y J, Zhang H G, Yin J H, Zhang H W, Chen J L, Wang W Q and Wu G H 2010 *J. Magn. Magn. Mater.* **322** 2251

[15] Troyanchuk I O, V.Bushinsky M, Karpinsky D V, Mantytskaya O S, Edotova V V and Prochnenko O I 2009 *J. Phys. Status Solidi B* **246** 8

[16] Zhou G H, Pan X and Zhu Y F 2013 *Acta Phys. Sin.* **62** 097502 (in Chinese)

[17] Yuan G L, Wing S, Liu J M and Liu Z G 2006 *Appl. Phys. Lett.* **89** 052905

[18] Pradhan S K, Das J, Rout P P, Mohanta V R, Das S K, Samantray S, Sahu D R, Huang J L, Verma S and Roul B K 2010 *J. Phys. Chem. S* **71** 1557

[19] A.Khomchenko V, Shvartsman V V, Borisov P, Kleemann W, Kiselev D, A, Bdikin I K, Vieira J M and Kholkin A L 2009 *Acta Mater.* **57** 5137

[20] Wang D H, Goh W C, Ning M and Ong C K 2006 *Appl. Phys. Lett.* **88** 212907

[21] Khomchenko V A and Kiselev D A 2007 *Appl. Phys. Lett.* **90** 242901

[22] Xu Q Y, Zai H F, Wu D, Qiu T and Xu M X 2009 *Appl. Phys. Lett.* **95** 112510

[23] Chang F G, Zhang N, Yang F, Wang S X and Song G L 2007 *J. Phy. D: Appl. Phys.* **40** 7799

[24] Kumar M and Yadav K L 2006 *J. Appl. Phys.* **100** 074111

[25] Zhang S X, Luo W J, Wang D L and Ma Y W 2009 *J. Mater. Lett.* **63** 1820

[26] Ruette B, Zvyagin S, Pyatakov A P, Bush A, Li J F, Belotelov V I, Zvezdin A K and Viehland D 2004 *Phys. Rev. B* **69** 064114

[27] Zhang S T, Lu M H, Wu D, Chen Y F and Ming N B 2005 *Appl. Phys. Lett.* **87** 262907

[28] Khomchenko V A, Karpinsky D V, Kholkin A, Sobolev N A, Kakazei G N, Araujo J P, Troyanchuk I.O, Costa B F O and Paixão J A 2010 *J. Appl. Phys.* **108** 074109

[29] Fullerton E E, Jiang J S and Bader S D 1999 *J. Magn. Magn. Mater.* **200** 392

[30] Das S R, Choudhary R N P, Bhattacharya P and Katiyara R S 2007 *J. Appl. Phys.* **101** 034104

[31] Lin Y H, Jiang Q H, Wang Y and Nan C W 2007 *Appl. Phys. Lett.* **90** 172507

[32] Jiang Q H, Ma J, Lin Y H, Nan C W, Shi Z and Shen Z J 2007 *Appl. Phys. Lett.* **91** 022914

[33] Zheng R K, Wen G H, Fung K K, and Zhang X X 2004 *J. Appl. Phys.* **95** 5244

[34] Kittel C 1986 *Introduction to Solid state Physics*, 6th edn. (New York, Chichester, Brisbane, Toronto, Singapore: John Wily & Sons) p. 447

[35] Palkar V R, John J and Pinto R 2002 *Appl. Phys. Lett.* **80** 1628

[36] Simõesa A Z, Garcia F G and Riccardi C S 2010 *J. Alloys Compd.* **493** 158

[37] Hu G D, Cheng X, Wu W B and Yang C H 2007 *Appl. Phys. Lett.* **91** 232909

[38] Wang S Y, Qiu X, Gao J, Feng Y, Su W N, Zheng J X, Yu D S and Li D J 2011 *Appl. Phys. Lett.* **98** 152902

[39] Li Y B, Yu J, Li J J, Zheng C D, Wu Y Y, Zhao Y, Wang M and Wang Y B 2011 *J. Mater. Sci: Matter Electron* **22** 323

[40] Ueda K, Tabata H and Kawai T 1999 *Appl. Phys. Lett.* **75** 4

[41] Wang N G, Cheng J, Pyatakov A, Zvezdin A K, Li J F, Cross L E and Viehland D 2005 *Phys. Rev. B* **72** 104434

[42] Ishibashi Y and Iwata M 2007 *Ferroelectrics* **354** 8